Monitoring of Tumor Growth and Vascularization with Repetitive Ultrasonography in the Chicken Chorioallantoic-Membrane-Assay.

Jonas Eckrich (Jonas.Eckrich@unimedizin-mainz.de)
Johannes Gutenberg Universitat Mainz https://orcid.org/0000-0001-5498-4031
Philipp Kugler
Department of Otorhinolaryngology, University Medical Center Mainz,
Christoph Raphael Buhr
Department of Otorhinolaryngology, University Medical Center Mainz
Benjamin Philipp Ernst
Department of Otorhinolaryngology, University Medical Center Mainz
Simone Mendler
Department of Otorhinolaryngology, University Medical Center Mainz
Jan Baumgart
Translational Animal Research Center of the Johannes Gutenberg-University Mainz
Juergen Brieger
Department of Otorhinolaryngology, University Medical Center Mainz
Nadine Wiesmann
Department of Otorhinolaryngology, University Medical Center Mainz

Research

Keywords: CAM assay, ultrasonography, in ovo imaging, method, tumor angiogenesis

Posted Date: August 14th, 2020

DOI: https://doi.org/10.21203/rs.3.rs-58821/v1

Abstract

Background: The chorioallantoic-membrane (CAM)-assay is used for versatile experimentation and eligible for the analysis of tumor angiogenesis, development and metastasis. In contrast to rodent xenograft models, the CAM-assay does not require breeding of immunodeficient strains for tumor experimentation due to native immunodeficiency. This allows xenografts to grow on the non-innervated CAM without pain or impairment for the embyo.

Taking into account the variability of multidirectional tumor growth, limited size monitoring capability is a major disadvantage of the CAM-assay as the enclosure of the tumor *in ovo* by the eggshell only allows for two-dimensional monitoring from above. The small size and the eggshell's shielding effect further challenge established imaging techniques. We report the eligibility of ultrasonographic imaging for repetitive monitoring of tumor growth and vascularisation in the CAM-assay.

Methods: Chicken eggs were placed in an incubator and cut open laterally on day three. On day seven a three-dimensional tumor was placed onto the CAM. Ultrasonographic imaging was then repetitively performed starting from day twelve. On day 14 the tumor was excised, fixed and histologically analyzed using light microscopy.

Results: Tumor volume and vascularization were repetitively visualized using a commercial ultrasonographic scanner, allowing a longitudinal monitoring of tumor growth and tumor angiogenesis. Findings in ultrasonographic imaging significantly correlated with results obtained in histological analysis.

Conclusion: Ultrasonography is cost efficient and widely available. It allows repetitive *in ovo* imaging and thereby enables visualization of tumor development. This increases the applicability of the CAM-assay as an alternative to xenograft rodent models in tumor research.

Background

Chicken eggs have been used as an experimental tool since the late 19th century (1). Further development of the method led to the identification of the chorioallantoic-membrane (CAM) as an easily accessible, well-vascularized anatomical structure suitable for versatile research. The CAM is an extraembryonic membrane that is formed by the partial fusing of the chick's chorion and its allantois during the embryonal development. Regarding its functions, the CAM can be considered as an equivalent to the mammalian placenta. Besides enabling the exchange of respiratory gases, it also draws calcium from the eggshell for the ebryonal bone development and regulates the acid-base homeostasis of the embryo as well as the reabsorption of ion and H_2O from the allantoic fluid (2).

Motivated by ethical concerns regarding the Draize rabbit eye test, Luepke identified the CAM as an alternative testing method in toxicological research (3). Made accessible for experimentation by partial removal of the eggshell, the CAM-assay was further established as a versatile research model for

analysis of angiogenesis (4), biomaterial research (5), toxicology (6–12), wound healing (13), bone regeneration (12) and tumor development (13).

For experimental tumor research, the CAM as a highly vascularized, non-innervated, extra-embryonic membrane is well suited for the engraftment of tumor cells. The high density of blood vessels creates an ideal milieu for tumor growth due to the ubiquitous supply of oxygen, nutrients, and growth factors (14). Different authors have already described the growth of solid tumors in the chicken egg and onto the CAM since the early 20th century (15). Ingrowth of blood vessels into the tumor has been described to start from day two to five after inoculation (16–19).

Due to the natural absence of a functioning cellular immune system in the hen's egg till day 14 of development, the implantation of xenografts onto the CAM does not require artificial induction of immunodeficiency (20).

In contrast, the sufficient immune system in rodent models leads to the rejection of xenografts. Consequently, rodent strains with severe immunodeficiency or a humanized immune system are a prerequisite for xenograft transplantation (21). Common xenograft rodent models comprise mice and rats with absence of B-cells (nude mice/rats) or severe combined immunodeficiency (SCID) (22–24).

Apart from ethical issues regarding the health of host animals, the use of rodent xenograft models requires specialized, very effortful and costly conditions suitable for keeping and breeding of host animals. In contrast, the CAM-assay is comparably simple methodology with moderate space requirements regarding incubation, allowing a high quantitative output without any need for excessive costs, personnel, or equipment (25, 26).

In rodent models, the implantation of the xenograft, monitoring of tumor growth, and -vascularization as well as any therapeutical interventions result in either stress, physical discomfort, pain or ultimately death for the host animal. In opposition to these constraints, the CAM has no nociceptive innervation. Moreover, the whole chick embryo is unable to experience pain until day 14 of incubation, due to the incomplete development of the nervous system (27).

In countries with high standards for animal care and research, using the CAM assay faces very low bureaucratic hurdles compared to *in vivo* rodent experiments since experimentation with the CAM assay does not require approval by a governmental organization nor an ethics committee for animal experimentation as long as the chickens are not hatched. (27, 28).

Multiple tumor entities have shown to grow sufficiently on the CAM (18, 29–31).

Observable parameters in tumor biology research are horizontal tumor size and vascularization of the growing tumor (32). The good accessibility of the CAM by removal of the eggshell, the chick's natural immunodeficiency, and the lower time expenditure are the obvious experimental advantages compared to *in vivo* xenograft rodent models. Without any tissue layer between the observer and the implanted tumor,

the malignant cells are fully accessible for observation and manipulation. Tumor angiogenesis and vasculogenesis can further be visualized using *in vivo* microscopy (13).

monitoring of three-dimensional tumor size and growth might be the main methodological limitation of the CAM-assay in the field of tumor experimentation. Although a direct view on the CAM is possible after partial shell removal, the microscopical evaluation of tumor size and tumor vascularization is limited by opacity of the surrounding eggshell as well as the autofluorescence of the solid tumor in fluorescence microscopy. In our experience, the tumor often grows deep into the CAM, resulting in a massive increase in tumor volume without major changes in lateral diameter. Furthermore, the movements of the chicken embryo further impede sufficient and reproducible microscopical investigation *in ovo*.

An end-point analysis can be realized by caliper measurements after excision or tumor fixation and preparation of histological slides. However, the high variation in directional growth as well as artefacts acquired during the fixation process limit the interpretability of these findings. Furthermore, an end-point analysis has obvious limitations for the interpretation of therapeutical effects in tumor experimentation especially in regard to the a.m. variability of tumor growth.

Imaging techniques like micro-computed tomography (CT) and micro-magnetic resonance imaging (MRI) might be suitable for three-dimensional visualization of the tumor. However, they are limited by their costs, availability of equipment as well as by the eligibility for the size and structure of the egg (33). The high density of the eggshell causes radio-opacity requiring the application of contrast agents for sufficient visualization of structures within the eggshell (34). These limitations can be overcome by intravascular application of markers and contrast agents, yet it is a challenging task due to the small diameter of the vessels on the CAM. Furthermore, intravascular application often results in excessive bleeding, leading to an increased dropout rate, impaired comparability and deteriorated experimental conditions as well as a potential inter-operator bias.

Thus, up until now, the absence of an accessible and sufficient three-dimensional imaging technique suitable for longitudinal visualization of tumor development limited the applicability of the CAM-assay for various investigations in the field of tumor research.

Ultrasonography utilizes a piezoelectric crystal which transmits and receives soundwaves usually in a range between 1 and 40 MHz. The live image is calculated by comparing the transmitted sound waves to the recurrent ones. Obvious key advantages are its widespread availability and its simple test setup. In addition, time and financial expenditure are far below equivalent imaging techniques like CT and MRI. Furthermore, ultrasonography does not influence or affect the experimental animal. Due to the absence of pain or suffering, no anesthesia is needed. In experimental research, ultrasonography has already been used successfully for tumor analysis in different *in vivo* models like mice (35). Furthermore, *in ovo* ultrasonography was utilized to investigate chicken embryology and especially the chick's heart development (33, 36). Taking these findings into consideration and searching for a suitable imaging method to quantify the size of tumors grown on the CAM in three dimensions, we tested the eligibility of repetitive color-duplex-ultrasonography for the analysis of tumor growth and tumor vascularization.

According to the Russell's and Burch's "Principles of Humane Experimental Technique" the reasonable use of the CAM-assay contributes to the refinement of animal experiments by minimizing pain and suffering of animals. As this methodology diversifies the applicability of the CAM–assay as a replacement for homologue rodent experiments, this model therefore meets the ethical obligations to reduce, refine, and replace (3Rs) animal usage in tumor research.

Specifically, this study evaluates the suitability of both single time as well as repetitive ultrasonography of tumors grown on the CAM for the quantification of tumor size, tumor growth and tumor vascularization. Comparative dropout rates were determined, and the results obtained in the ultrasonographic measurements were matched to the subsequent immunohistochemical analysis regarding tumor vascularization and tumor size. Finally, an exemplary comparative mathematical analysis of the costs of the *in ovo* tumor model and the *in vivo* tumor model was conducted.

Methods

Eggs and tumor development

White Leghorn hens' eggs were placed horizontally in an incubator (Brutmaschinen-Janeschitz GmbH, Hammelburg, Deutschland) at 37.5 °C. On day 3 of incubation, 6 ml albumen was removed by aspiration with a sterilized syringe. The shell was opened with sterilized scissors and parts of the shell were removed. After opening the eggshells, the aperture was covered with PARAFILM→ (Bemis Company Inc., Neenah, Wisconsin, USA) to avoid evaporation. Cultivation of the liver cancer HuH7 tumor cells (37) on the CAM started by day 7.

One day before placement onto the CAM the HuH7 tumor cells were harvested by tryptic digestion from the cell culture flask, counted with a Neubauer counting chamber, and distributed in 1.5 ml tubes (5 Mio. cells per egg). After centrifugation at 1400 rpm for 10 min the supernatant was removed, and the cell pellet was subsequently suspended in ice cooled Matrigel™ (Corning™, Brumath, France). The five million cells were then incubated for 30 min on a 6-well plate at 37.5 °C (Greiner, bio-one International GmbH, Kremsmünster, Austria) until the Matrigel™ had hardened to a firm consistency. The 3D cell culture was then covered with culture medium, and finally incubated overnight.

Upon placement on the CAM a well vascularized spot was selected and carefully incised using a single-use-scalpel (Feather, Dr. Junghans Medical GmbH, Bad Lausick, Germany). Afterwards the 3D culture was placed onto the incision and 20 µl of Matrigel™ was pipetted onto the culture for protection against cell desiccation and immobilization on the CAM. The eggs were then incubated as mentioned above.

Ultrasonography

Starting from day 12 of incubation (5 days after tumor inoculation) the GE Healthcare Ultrasound LOGIQ E9 (GE Healthcare Little Chalfont, UK) 15 MHz linear transducer was used in the B-Mode (Gain 35) for

ultrasonographic imaging (Fig. 1). Instead of ultrasound gel the space between the CAM and shell opening was filled with an average of 4 ml Sodium chloride (NaCl) 0.9% to allow transduction of ultrasound waves. Tumors were then visualized in both longitudinal and transversal axes to enable a three-dimensional quantification of the tumor size. The respective image was frozen using the “Freeze” function and the tumor length, width and thickness was measured and documented.

Color-duplex-sonography was carried out using the same methodology while the built-in Duplex mode enabled visualization of the vessels within the tumor. Video sequences were saved for offline analysis.

For repetitive measurements, the same procedure was carried out on days 12, 13, and 14 respectively. The NaCl 0.9% solution was removed after each measurement using an electrical pipette (INTEGRA Biosciences GmbH, Biebertal, Germany) with a 10 ml sterile tube (Greiner CELLSTAR® serological pipette, Greiner AG, Bischofsheim, Germany)

Immunohistochemistry

After completion of the study protocol the embryo was sacrificed by decapitation. The CAM bearing the tumor was then excised with sterilized surgical scissors and placed onto filter paper stripes. The longitudinal and transversal axis were marked on the paper, the tumor-bearing CAM was transferred into a plastic cassette (Carl Roth GmbH + Co. KG, Karlsruhe, Germany), immobilized and put into a formalin solution (4%) (VWR International bvba, Leuven, Belgium) for 24 h. Afterwards, the plastic cassette was removed from the 4% formalin solution, washed three times with purified water for 20 min each, and incubated in isopropanol solution with increasing concentrations (80%/90%/100%) for 1 h each. The cassette was then washed with purified water and incubated in xylene (AppliChem GmbH, Darmstadt, Germany) for 24 h. Each specimen was imbedded in paraffin and cut into 5 µm slides with a microtome (Leica CM1900, Leica Biosystems Nussloch GmbH, Nußloch, Germany) according to the marking previously placed on the slides.

For hematoxylin and eosin (HE) stains, Paraffin was removed from the slide and the specimen was incubated in Mayer’s Hemalum Roth (Carl Roth GmbH + Co. KG, Karlsruhe, Germany) for 5 min. Subsequently, each slide was again washed in purified water and incubated in eosin (Merck KGaA, Darmstadt, Germany) for 2 min. Slides were then incubated in isopropanol solution with increasing concentrations (80%/90%/100%) for 2 min each and xylene for 10 min. Finally, slides were prepared for microscopy by embedding the specimen in Eukitt® (Sigma-Aldrich, St. Louis, Missouri, USA).

Immunohistochemical staining for alpha smooth muscle actin (Alpha-SMA) allowed visualization of vessels within the CAM. Slides were dewaxed with xylene and isopropanol solutions with decreasing concentrations (100%/90%/80%/70%) for 5 min each and cooked in citrate buffer (pH 6.0) for 30 min. After preparation slides were incubated with monoclonal Alpha-SMA antibodies (A2547, Sigma-Aldrich, St. Louis, Missouri, USA) dissolved in (1/1500) phosphate-buffered-saline (PBS) + 1% bovine serum albumin (BSA). As secondary antibody biotinylated polyclonal goat anti-mouse immunoglobulin (P 0447,

Dako Denmark A/S, Glostrup, Denmark) was added and visualized using horseradish peroxidase-conjugated streptavidin (1/250) (Dako Denmark A/S, Glostrup, Denmark). Finally, slides were again prepared for microscopy by embedding the specimen in Eukitt ® (Sigma-Aldrich, St. Louis, Missouri, USA).

Microscopical Analysis

Microscopical slides were investigated using the Nikon Eclipse TE2000 Inverted Microscope (Nikon Corp. Chiyoda, Japan) and digitalized by transferring the image from the inbuilt camera system (Nikon's DS-Fi3, Nikon Corp. Chiyoda, Japan) into Nikon’s analysis software NIS-Elements (Nikon Corp. Chiyoda, Japan).

Data Management and Off-Line Analysis

Tumor diameters, measured in ultrasonographic images were transferred into EXCEL sheets (Microsoft Corp., Redmond, WA, USA). For determination of tumor vascularization, the video files of color-duplex-ultrasonography were exported and the presence and intensity of vessels in the CAM was rated in a three step rating system (0 = no intratumoral vascularization, 1 = moderate intratumoral vascularization, 2 = intense intratumoral vascularization) by two blinded otorhinolaryngological specialists (J.E., B.E.), experienced in clinical ultrasonographic diagnostics independently. Ratings were then evaluated for concordance and reevaluated in case of discrepancy until a clinical consensus was reached between both investigators. Results were again inserted into EXCEL sheets.

The images of the HE-stained tumors were used to determine tumor size by measuring the diameters in both sagittal and transversal planes by laboratory personnel blinded to the results of the ultrasonographic imaging. To evaluate tumor vascularization Alpha-SMA staining was used. Similarly, to ultrasonographic imaging, the amount of intratumoral vascularization was quantified in a three step rating system (0 = no intratumoral vascularization, 1 = moderate intratumoral vascularization, 2 = intense intratumoral vascularization).

As tumors grow in a rounded shape, calculation of estimated tumor volumes from the three diameters obtained in ultrasonography was realized using the triaxial ellipsoid formula (V = 4/3 x Pi x [0.5 x d1{sagittal}] x [0.5 x d2{transversal} x0.5 x d3{coronar}]).

For the longitudinally cut histological slides the approximated two-dimensional tumor area could be calculated by using the ellipsis formula (A = Pi x d1[sagittal] x d2[transversal]).

To further allow comparability of size quantification by ultrasonography with the size determined by histological analysis, the tumor area in ultrasonography was determined by insertion of the longitudinal and sagittal diameters in the above mentioned ellipsis formula.

Success rates of tumor development were determined by calculating the percentage of solid tumors on the CAM on day 11 of incubation in relation to the number of eggs incubated on day 0. Accordingly, success rates regarding the possibility of ultrasonographic imaging in all three dimensions were calculated by dividing the eggs in which application of ultrasonography was possible by the number of CAMs with solid tumors.

Statistical Analysis

Column statistics as well as comparative statistical analysis were carried out using GraphPad Prism™ (GraphPad Software, Inc., La Jolla, CA, USA). Besides column statistics (mean, median, range, standard deviation, standard error, Gaussian distribution and confidence intervals 95) comparative analysis was carried out as follows: As most data sets regarding tumor volume and vascularization did not show a Gaussian distribution, correlation between tumor sizes determined in ultrasonography as well as histology was determined using the Spearman-correlation.

For longitudinal analysis of tumor growth as well as changes in vascularization determined in ultrasonography the Friedman repeated measures test was used to determine whether volumes significantly differed between the days of observation.

Differences in survival after repetitive ultrasonography were determined using the log-rank test as well as the Gehan-Breslow-Wilcoxon test.

Cost Analysis

For comparing the costs of the CAM assay to rodent tumor models, the average costs for mice represented by the Crt:NU(NCr)-Foxn1nu/nu line (male, 6 weeks old) for a duration of 14 days were calculated. As source data the median prices for chicken eggs of the main distributer in the specific region (Bio-Aufzucht LSL Rhein-Main GmbH, Dieburg, Germany) as well as mice according to the 3 available distributers for nude mice in the specific region (Janvier Labs, Paris, France; Charles River Wiga GmbH, Sulzfeld, Germany; Envigo RMS GmbH, Roßdorf, Germany) were taken into account. Costs for transport as well as the gross running costs, provided by Translational Animal Research Center, University Medical Center of the Johannes Gutenberg-University Mainz, Mainz, Germany were considered. The cost of keeping animals in our facility is on average the price of equivalent German facilities known to us. An amount of 75 eggs as well as 25 mice was taken as the average sample size.

Results

CAM-Assay and Tumor Development

As shown in Fig. 2 due to an extensive experience with this model we were able to retrospectively analyze a very high number of eggs (n = 1044) used for different studies in our lab. Regarding the success rate of

inoculation of (HUH7) tumors on the CAM, without any intervention till day 11, 52.68% (± 11.89%) of these 1044 eggs showed viability as well as sufficient ingrowth of the transplanted tumor.

For this specific study regarding ultrasonographic analysis 189 eggs were randomly selected. Repetitive ultrasonography was performed on 36 eggs. 54.00% (± 29.47%) of the randomly selected eggs had a tumor positioning on the CAM eligible for sufficient ultrasonographic imaging and measuring of all three tumor diameters respectively.

Tumor Size

In ultrasonographic analysis the median tumor volume on the CAM determined on day 14 was 0.075 cm^3 (± 0.072 cm^3). Accordingly, the calculated two-dimensional tumor size was 0.69 cm^2 (± 0.4355 cm^2). Measurement of tumor size in histology determined an average tumor size of 0.096 cm^2 (± 0.052 cm^2). For both methodological entities the measured tumor sizes correlated significantly (r = 0.49, P[twotailed] = 0.0047) in the Spearman test.

Tumor Vascularization

Tumor vascularization could be visualized in 81.0% of eggs on day 14 using color-duplex-ultrasonography. 9.5% did not show any intratumoral vascularization, 28.6% were ranked as moderate intratumorally vascularized, and 61.9% showed an intense intratumoral vascularization. Analysis of histological slides showed vessel formation within the tumor tissue in 90.5% of all tumors analyzed. Comparable to the results obtained by ultrasonography 9.5% did not show any intratumoral vascularization. In 45% of cases the intratumoral vascularization was ranked as moderate and 47% of evaluated slides showed an intense intratumoral vascularization. Comparative analysis with the Spearman test regarding the intensity of vascularization within the tumor tissue correlated significantly (r = 0.65, P[twotailed] < 0.0001) between ultrasonography and histological analysis.

Repetitive Ultrasonography Measurement

Repetitive ultrasonographic measurements on day 12, 13 and 14 of incubation revealed a significant increase of tumor volume within the timeframe of observation as shown in Fig. 5 (P < 0,0001). From day 12 to day 13 the tumors showed an average size increase of 129.5% while from day 13 to day 14 an average size increase of 45.5% was evaluated. Changes between the three days were significantly different as calculated with the Friedman test (p = 0.0048). Repetitive evaluation of tumor vascularization in ultrasonography showed an increasing perfusion of tumor tissue over the observed period of three days.

Survival Analysis:

For repetitive ultrasonography, a log-rank test was performed to determine whether repetitive ultrasonography caused a significantly impaired survival when compared to untreated controls in the timeframe from day 12–14 of incubation. The differences in log-rank as well as the Gehan-Breslow-Wilcoxon test did not show significant differences for survival between the two groups (log-rank test [P = 0.42]; Gehan-Breslow-Wilcoxon test [P = 0.41]) as shown in Fig. 6.

Cost Calculation:

Calculation of costs regarding different methodologies is difficult due to diverse prices for animals and housing in different institutions. Furthermore, additional costs like tumor cells, tools for preparation, housing or infrastructure may differ depending on the specific experimentation setup. Therefore, costs for cages, incubators, tumor cells, cell-medium or further equipment were not taken into consideration.

Furthermore, since we currently do not perform any experimentation with subcutaneously implanted tumors in rodents in our laboratory, inoculation rates from published data using liver cancer cell lines (38–42) were utilized as comparative data. As shown in Table 1 median costs for a hen's egg were approximately 2.1 € while a single nude mouse *(Crt:NU(NCr)-Foxn1nu/nu)* has an average cost of 53.8 € per animal. Of all the eggs incubated after shipment, 53% show successful tumor inoculation on day 11 after incubation. Though solid data regarding ingrowth of subcutaneously implanted tumors in scientific articles is scarce and has shown a large variety ranging from below 50% (41) to 92% (40). The median inoculation rate was estimated around 77.5% (median value considering literature analysis).

Taking these numbers into consideration and adding the running costs like food and housing for two weeks into consideration, the average price for an egg bearing a tumor on the CAM is 3.9 € while a mouse with a subcutaneous tumor will cost approximately 69.5 € per animal **(Table 1).**

Table 1.

	CAM Assay	Nude mouse[1] (male, six weeks old)
Median costs/animal [€]	2.06[2]	53.84[3]
Successful tumor growth [%]	53	78[4]
Running costs / week [€]	0.02	2.94[5]
Calculated average cost/successful tumor (*in ovo/ in vivo*) [€]	3.91	69.47

[1] Resembled by the *Crt:NU(NCr)-Foxn1nu/nu* strain

[2] Median costs/ egg (including transport costs) of the main distributer of Hens-Eggs in the specific region (Bio-Aufzucht LSL Rhein-Main GmbH, Dieburg, Germany)

[3] Median Costs for a male, six weeks old *Crt:NU(NCr)-Foxn1nu/nu* mouse according to the 3 available distributers for nude mice in the specific region (Janvier Labs, Paris, France; Charles River Wiga GmbH, Sulzfeld, Germany; Envigo RMS GmbH, Roßdorf, Germany)

[4] (Gong et al., 2019; Huang et al., 2012; Robertson et al., 2016; Xu et al., 2019; Zhang et al., 2020)

[5] Resembled by the average running costs for SCID mice in our specific institution (Translational Animal Research Center, Gutenberg University Mainz)

Discussion

The CAM-assay has been established for many scientific purposes as an alternative method in comparison to homologue rodent experiments. In tumor experimentation however, rodent experiments with subcutaneously implanted xenografts are still considered the “gold standard” regarding the evaluation of tumor treatment. In our working group the CAM-assay is regularly performed for tumor experimentation. By implication, therefore we were able to develop a rich experience and expertise using this specific model. As shown in Fig. 2, **52**.68% (± 11.89%) of the eggs incubated with tumors showed viability as well as sufficient ingrowth of the transplanted tumor on day 11. Tumor take rates reported in scientific literature show a large variety and range from 70–80% (18, 31, 43) to much lower inoculation rates of around 45% (44) depending on the specific tumor entity used for investigation. Unfortunately, in many studies it is difficult to see the true dropout rates as only positive ingrowth rates or treatment effects are reported without any quantification of dropout rates.

Retrospective analysis of our study protocols showed no significant decrease of dropout rates or increase of tumor take rates over time. Yet some batches of eggs show elevated dropout rates compared to others.

This effect might be attributable to different fertilization rates or possible damage during transportation. In our experience apart from death of the chicken embryo, luxation or movement of the tumor on the CAM due to growth of the embryo as well as insufficient ingrowth of tumors are the main reasons for dropout from the experimentation protocol. Eligibility for ultrasonographic analysis is heavily determined by the placement of the tumor on the CAM. As shown in Fig. 2 approximately 54.0% (± 29.47%) of the eggs bearing an inoculated tumor on the CAM meet this criterion and ultrasonographic imaging and measuring was possible in all three dimensions.

Different working groups have published data proclaiming the evaluation of tumor growth using the CAM-assay. In many published articles however, tumor growth is only measured twodimensionally or estimated using surrogate parameters like bioluminescence (31). Furthermore, end-point-analysis in the form of size measuring (45), cell count in flow cytometry of digested tumors, or weight measurements (46) have been utilized or the determination of tumor size.

Interestingly, accurate three-dimensional imaging has rarely been published. Kim et al. used MRI imaging for anatomical studies (47) and Henning et al. used contrast agents to visualize the chick anatomy *in ovo* (34). Recently, Huang et al. compared the quantification of ultrafast ultrasound microvessel imaging (UMI) with power Doppler imaging (48). However, as only a singular time point was analyzed repetitive longitudinal monitoring of tumor size and monitoring of tumor growth have not been described.

As shown in Fig. 5 we were able to repetitively analyze tumor size and vascularization using a commercial ultrasonographic scanner. As ultrasound is commonly used in clinical diagnosis, many scientific institutions attached to hospitals have access to this imaging technique. Repetitive visualization of tumor vascularization makes longitudinal quantification of tumor perfusion possible. This is immensely useful since therapeutical effects on intratumoral vessels (e.g. during radiotherapy or after application of anti-angiogenic drugs) could be longitudinally quantified (39, 49)

With regard to the assessment of the tumor size using ultrasonographic imaging compared to the histological sectional image, we expected great inaccuracies due to deviations in the sectional plane, artefacts and shrinkage during the preparation of histological slides. Nevertheless, tumor size in a two-dimensional sectional plane significantly correlated between ultrasonographic imaging and histological analysis. The average plane of the tumors measured in histological slides showed only approximately 13% of the tumors original plane, measured in ultrasonography. Hence we assume an intense shrinkage of the during the fixation process. This is further indicated by the fact that photographic documentation of the tumors shows diameters similar to ultrasonographic measurements **(**Fig. 3**)** and accuracy regarding the ultrasonographic measurements was further evaluated and verified **(Supplementary Information S2)** indicating an inaccuracy of approximately 1%. Nevertheless, although the inclusion of the third observation level was only possible in ultrasonographic diagnostics, a significant correlation of the three-dimensional tumor volume with the tumor area determined in the histological slide was detected ($r = 0.48$, P[two-tailed] = 0.0059) **(Supplementary Information S3).** By implication, therefore we strongly believe that tumor size can be sufficiently monitored using ultrasonographic imaging.

Additional to monitoring of the tumor size we were able to show that tumor vascularization can be visualized using a commercial ultrasonographic scanner. Similar to the findings reported by Huang et al. (48) tumor vascularization also correlated with the findings obtained in histological analysis as shown in Fig. 4. Though we were surprised by the high quantity of size increase as shown in Fig. 5, other working groups also described a phase of rapid tumor growth after penetration of the tumor by new blood vessels (50). These findings are further supported by the increase of detectable vascularization in color-duplex-ultrasonography suggesting an intensifying supply of oxygen and nutrients within the tumor.

In contrast to radiological imaging like CT, ultrasound represents a cost-efficient alternative without the effects of ionizing radiation on either the egg or the CAM. Whilst MRI has no radiation, the increased cost factor as well as impaired imaging resolution due to movement of the embryo are obvious limitations (47) compared to ultrasonography. Since the 3–5 ml of NaCl necessary for transduction of ultrasound waves might have a negative influence regarding dropout rates as well as tumor development we analyzed the overall survival of eggs undergoing repetitive ultrasonographic imaging as well as untreated eggs for the duration of imaging. As shown in Fig. 5 no significant differences in the dropout rate were monitored during the respective timeframe.

Obviously, quality of imaging could be improved by using high resolution imaging like ultrafast ultrasound microvessel imaging (48). Yet, ultra-high to low frequency imaging systems are highly specialized research equipment not available in most institutions while commercial ultrasonographic imagery is pretty much omnipresent in clinical patient care. Furthermore, the comparison of tumor size between ultrasonography and histological slides has obvious drawbacks like folding artefacts, shrinkage of tissue and deviations in the sectional plane. As tumors inoculated in the CAM often show extensive hematomas and further regularly show intense ingrowth of the CAMs stromal cells into the tumor tissue, growth of the tumor might not be attributable to growth of tumor tissue alone but rather by a bidirectional infiltration of tumor tissue and CAM (27). Yet apart from stromal cell invasion (51) measuring of tumor size bears similar chances of inaccurate measurements in subcutaneously implanted tumors in rodents as well. Though subcutaneously implanted tumors do rarely infiltrate the adjacent tissue e.g. muscle and stroma, measuring with calipers still bares the possibility of inaccuracy due to deviations in transtumoral measuring axis and inter-operator variability (52, 53). The accuracy of ultrasonographic analysis was further evaluated in experimental setting resembling the experimental conditions of *in ovo* sonography **(Supplementary Information S2)** indicating an inaccuracy of approximately 1%.

Today mouse models have been established as the gold standard for *in vivo* experimentation. Their widespread availability as well as their relatively low housing costs compared to larger laboratory animals, fast reproduction rate and the availability of multiple knock out and transgenic lines make them the favorable animal model for most researchers. According to the “Bundesministerium für Ernährung und Landwirtschaft” (German Ministry of Food and Agriculture) in 2017, 1.37 million mice were used for animal experimentation in Germany alone making them by far the most extensively used vertebrate species in research today. Xenografts are usually implanted subcutaneously, due to easy accessibility and the possibility of three-dimensional size monitoring using calipers or advanced imaging like CT, MRI,

or bioluminescence detection (54). In contrast to the CAM-assay, in which neither the CAM nor the embryo are nociceptive, any evaluation of the tumor size in the mouse model results in stress or discomfort through repetitive handling, movement restriction or sedation. An obvious disadvantage of *in ovo* experimentation however is the short observational window. Whilst in rodent experiments long therapeutic timeframes can be repetitively observed, *in ovo* experimentation will ultimately be terminated by the hatching of the chicken on day 21. In our working group we only evaluated tumor growth till day 14 due to ethical concerns and the occurrence of nonspecific inflammatory reactions typically starting after 15 days of incubation (27). Nevertheless, other working groups evaluated tumor development till day 20 of incubation (55). Contrarily tumors on the CAM grow much faster than equivalent tumors subcutaneously implanted into mice and vessel ingrowth (50) as well as tumor metastasis was successfully determined using the CAM-assay (56). Hu et al. were able to show that renal cell carcinoma xenografts inoculated on the CAM maintain the same tumor growth pattern and metastatic behavior as observed in mice (55). Some research groups were able to demonstrate parallels regarding tumor size for different tumor entities in comparative experiments with eggs and mice (45, 57). Nevertheless, an investigation of interactions between malignant tissue and immune cells is currently only possible in mouse models with specifically modified or humanized immune systems. Finally, in our experience only very few chicken specific antibodies are currently commercially available. With increasing popularity of this model however this might change in the near future. In conclusion the CAM-assay is a versatile model offering a translational significance equal to equivalent rodent experiments for many scientific questions in the field of tumor research.

Although chicken embryos are not considered independently living animals in most countries and therefore meet the criteria of the 3R principle, obvious ethical questions regarding the replacement of an animal experiment with another experiment remain and have to be addressed carefully. However, even when addressing this controversial question, due to the lack of nociception in the CAM-assay, this methodology is ethically preferable to homologous mouse experiments.

Finally, as exemplarily shown in Table 1 the costs for a sufficiently ingrown tumor suitable for experimentation highlight the significantly increased cost efficiency of the CAM-assay compared to rodent experiments. Even though other institutions might be able to obtain mice for cheaper prices, keep them at lower running costs and even though additional factors like costs for tumor preparation, equipment and laboratory utensils have been left out of consideration the CAM-assay has the obvious economic benefits even though rates of tumor inoculation might be lower. Furthermore, keeping chicken embryos does not require official approval to keep and breed experimental animals. For example, this model can be used in laboratories that do not have an animal experimental unit.

Conclusion

In conclusion repetitive ultrasonography is suited for sufficient quantification of tumor size and intratumoral vascularization without increased dropout rates. Apart from obvious advantages like cost efficiency and widespread availability it is the first time repetitive longitudinal tumor imaging *in ovo* was

successfully visualized without the help of surrogate parameters like bioluminescence. Therefore, this methodology further diversifies the applicability of the CAM–assay as an alternative methodology to rodent tumor experimentation.

Abbreviations

CAM – chorioallantoic-membrane

SCID – Severin combined immunodefiency

CT – Computer tomography

MRI – magnetic resonance imaging

3Rs – reduce, refine, replace

NaCl – sodium chloride

HE – hematoxilin and eosin

Alpha-SMA – alpha smooth muscle actin

PBS – phosphate buffered saline

BSA – bovine serum albumin

UMI – ultrasound microvessel imaging

Declarations

Ethics approval and consent to participate:

Not applicable

Consent for publication:

Not applicable

Availability of data and materials:

All data generated or analysed during this study are included in its supplementary information files.

Competing interests:

The authors declare that they have no competing interests.

Funding:

No third party funding was utilized for the design of the study and collection, analysis and interpretation of data and in writing the manuscript.

Author Contributions:

J.E. made substantial contributions to the conception of the work. He further was involved in acquisition, analysis and interpretation of data. Finally, he drafted the manuscript and approved the submitted version. He further agreed both to be personally accountable for the author's own contributions and for the accuracy and integrity of any part of the work. As the corresponding author he claims responsible for ensuring that all listed authors have approved the manuscript before submission. He declares that all scientific writers and anyone else who assisted with the preparation of the manuscript content are properly be acknowledged, along with their source of funding. He further states that no authors on earlier versions have been removed and no new authors were added.

P.K. was involved in acquisition, analysis and interpretation of data. He further participated in drafting and revising of the manuscript and approved the submitted version. He further agreed both to be personally accountable for the author's own contributions and for the accuracy and integrity of any part of the work.

C.R.B. was involved in acquisition, analysis and interpretation of data. He further participated in drafting and revising of the manuscript and approved the submitted version. He further agreed both to be personally accountable for the author's own contributions and for the accuracy and integrity of any part of the work.

B.P.E. was involved in analysis and interpretation of data. He substantively revised the manuscript and approved the submitted version. He further agreed both to be personally accountable for the author's own contributions and for the accuracy and integrity of any part of the work.

S.M. was substantially involved in acquisition and analysis of data. She further paticipated revising the methods section of the manuscript and approved the submitted version. She agreed both to be personally accountable for the author's own contributions and for the accuracy and integrity of any part of the work.

J.Ba. was involved in acquisition and interpretation of data. He substantively revised the manuscript and approved the submitted version. He further agreed both to be personally accountable for the author's own contributions and for the accuracy and integrity of any part of the work.

J.Br. made substantial contributions to the design of the work. He further was involved in the interpretation of data and substantively revised the manuscript. He approved the submitted version and agreed both to be personally accountable for the author's own contributions and for the accuracy and integrity of any part of the work.

N.W. made substantial contributions to the conception and design of the work she substantially participated in the acquisition, analysis, and interpretation of data and the drafting process of this manuscript. She agreed both to be personally accountable for the author's own contributions and for the accuracy and integrity of any part of the work.

Aknowledgements:

Not applicable

References

1. Gerlach L. Über neue Methoden auf dem Gebiet der experimentellen Embyrologie. Anatomischer Anzeiger Centralblatt für die gesamte wissenschaftliche Anatomie Amtliches Organ der Anatomischen Gesellschaft. 1887:pp. 583–609.
2. Gabrielli MG, Accili D. The chick chorioallantoic membrane: a model of molecular, structural, and functional adaptation to transepithelial ion transport and barrier function during embryonic development. J Biomed Biotechnol. 2010;2010:940741.
3. Luepke NP. Hen's egg chorioallantoic membrane test for irritation potential. Food Chem Toxicol. 1985;23(2):287-91.
4. Ribatti D. The chick embryo chorioallantoic membrane in the study of tumor angiogenesis. Rom J Morphol Embryol. 2008;49(2):131-5.
5. Baiguera S, Gonfiotti A, Jaus M, Comin CE, Paglierani M, Del Gaudio C, et al. Development of bioengineered human larynx. Biomaterials. 2011;32(19):4433-42.
6. Blasi P, Schoubben A, Traina G, Manfroni G, Barberini L, Alberti PF, et al. Lipid nanoparticles for brain targeting III. Long-term stability and in vivo toxicity. Int J Pharm. 2013;454(1):316-23.
7. E. GMS. The influence of silver nanoparticles on chicken embryo development and bursa of Fabricius morphology. Journal of Animal and Feed Sciences. 2006; 15, Suppl. 1(2006):111–4.
8. Kue CS, Tan KY, Lam ML, Lee HB. Chick embryo chorioallantoic membrane (CAM): an alternative predictive model in acute toxicological studies for anti-cancer drugs. Exp Anim. 2015;64(2):129-38.
9. Roman D, Yasmeen A, Mireuta M, Stiharu I, Al Moustafa AE. Significant toxic role for single-walled carbon nanotubes during normal embryogenesis. Nanomedicine. 2013;9(7):945-50.
10. Urbanska K, Pajak B, Orzechowski A, Sokolowska J, Grodzik M, Sawosz E, et al. The effect of silver nanoparticles (AgNPs) on proliferation and apoptosis of in ovo cultured glioblastoma multiforme (GBM) cells. Nanoscale Res Lett. 2015;10:98.
11. Vinardell MP, Mitjans M. Alternative methods for eye and skin irritation tests: an overview. J Pharm Sci. 2008;97(1):46-59.
12. Moreno-Jimenez I, Hulsart-Billstrom G, Lanham SA, Janeczek AA, Kontouli N, Kanczler JM, et al. The chorioallantoic membrane (CAM) assay for the study of human bone regeneration: a refinement animal model for tissue engineering. Sci Rep. 2016;6:32168.

13. Ribatti D. The chick embryo chorioallantoic membrane as a model for tumor biology. Exp Cell Res. 2014;328(2):314-24.
14. Nowak-Sliwinska P, Segura T, Iruela-Arispe ML. The chicken chorioallantoic membrane model in biology, medicine and bioengineering. Angiogenesis. 2014;17(4):779-804.
15. Murphy JB, Rous P. The Behavior of Chicken Sarcoma Implanted in the Developing Embryo. J Exp Med. 1912;15(2):119-32.
16. Dohle DS, Pasa SD, Gustmann S, Laub M, Wissler JH, Jennissen HP, et al. Chick ex ovo culture and ex ovo CAM assay: how it really works. J Vis Exp. 2009(33).
17. Knighton D, Ausprunk D, Tapper D, Folkman J. Avascular and vascular phases of tumour growth in the chick embryo. Br J Cancer. 1977;35(3):347-56.
18. Kunz P, Schenker A, Sahr H, Lehner B, Fellenberg J. Optimization of the chicken chorioallantoic membrane assay as reliable in vivo model for the analysis of osteosarcoma. PLoS One. 2019;14(4):e0215312.
19. Kunzi-Rapp K, Genze F, Kufer R, Reich E, Hautmann RE, Gschwend JE. Chorioallantoic membrane assay: vascularized 3-dimensional cell culture system for human prostate cancer cells as an animal substitute model. J Urol. 2001;166(4):1502-7.
20. Janse EM, Jeurissen SH. Ontogeny and function of two non-lymphoid cell populations in the chicken embryo. Immunobiology. 1991;182(5):472-81.
21. Richmond A, Su Y. Mouse xenograft models vs GEM models for human cancer therapeutics. Dis Model Mech. 2008;1(2-3):78-82.
22. Bosma GC, Custer RP, Bosma MJ. A severe combined immunodeficiency mutation in the mouse. Nature. 1983;301(5900):527-30.
23. Colston MJ, Fieldsteel AH, Dawson PJ. Growth and regression of human tumor cell lines in congenitally athymic (rnu/rnu) rats. J Natl Cancer Inst. 1981;66(5):843-8.
24. Maruo K, Ueyama Y, Kuwahara Y, Hioki K, Saito M, Nomura T, et al. Human tumour xenografts in athymic rats and their age dependence. Br J Cancer. 1982;45(5):786-9.
25. Lokman NA, Elder AS, Ricciardelli C, Oehler MK. Chick chorioallantoic membrane (CAM) assay as an in vivo model to study the effect of newly identified molecules on ovarian cancer invasion and metastasis. Int J Mol Sci. 2012;13(8):9959-70.
26. Vargas A, Zeisser-Labouebe M, Lange N, Gurny R, Delie F. The chick embryo and its chorioallantoic membrane (CAM) for the in vivo evaluation of drug delivery systems. Adv Drug Deliv Rev. 2007;59(11):1162-76.
27. Ribatti D. The chick embryo chorioallantoic membrane (CAM). A multifaceted experimental model. Mech Dev. 2016;141:70-7.
28. DIRECTIVE 2010/63/EU OF THE EUROPEAN PARLIAMENT AND OF THE COUNCIL of 22 September 2010 on the protection of animals used for scientific purposes (2010) Available at: https://eur-lex.europa.eu/LexUriServ/LexUriServ.do?uri=OJ:L:2010:276:0033:0079:EN:PDF (21 April 2020).

29. Ferician O, Cimpean AM, Avram S, Raica M. Endostatin Effects on Tumor Cells and Vascular Network of Human Renal Cell Carcinoma Implanted on Chick Embryo Chorioallantoic Membrane. Anticancer Res. 2015;35(12):6521-8.
30. Marzullo A, Vacca A, Roncali L, Pollice L, Ribatti D. Angiogenesis in hepatocellular carcinoma: an experimental study in the chick embryo chorioallantoic membrane. Int J Oncol. 1998;13(1):17-21.
31. Rovithi M, Avan A, Funel N, Leon LG, Gomez VE, Wurdinger T, et al. Development of bioluminescent chick chorioallantoic membrane (CAM) models for primary pancreatic cancer cells: a platform for drug testing. Sci Rep. 2017;7:44686.
32. Teitz T, Stanke JJ, Federico S, Bradley CL, Brennan R, Zhang J, et al. Preclinical models for neuroblastoma: establishing a baseline for treatment. PLoS One. 2011;6(4):e19133.
33. McQuinn TC, Bratoeva M, Dealmeida A, Remond M, Thompson RP, Sedmera D. High-frequency ultrasonographic imaging of avian cardiovascular development. Dev Dyn. 2007;236(12):3503-13.
34. Henning AL, Jiang MX, Yalcin HC, Butcher JT. Quantitative three-dimensional imaging of live avian embryonic morphogenesis via micro-computed tomography. Dev Dyn. 2011;240(8):1949-57.
35. Fruth K, Weber S, Okcu Y, Noppens R, Klein KU, Joest E, et al. Increased basic fibroblast growth factor release and proliferation in xenotransplanted squamous cell carcinoma after combined irradiation/anti-vascular endothelial growth factor treatment. Oncol Rep. 2012;27(5):1573-9.
36. Pugh CR, Peebles ED, Pugh NP, Latour MA. Ultrasonography as a tool for monitoring in ovo chicken development. 1. Technique and morphological findings. Poult Sci. 1993;72(12):2236-46.
37. Nakabayashi H, Taketa K, Miyano K, Yamane T, Sato J. Growth of Human Hepatoma-Cell Lines with Differentiated Functions in Chemically Defined Medium. Cancer Res. 1982;42(9):3858-63.
38. Gong T, Ning X, Deng Z, Liu M, Zhou B, Chen X, et al. Propofol-induced miR-219-5p inhibits growth and invasion of hepatocellular carcinoma through suppression of GPC3-mediated Wnt/beta-catenin signalling activation. J Cell Biochem. 2019;120(10):16934-45.
39. Huang G, Chen L. Tumor vasculature and microenvironment normalization: a possible mechanism of antiangiogenesis therapy. Cancer Biother Radiopharm. 2008;23(5):661-7.
40. Robertson RT, Gutierrez PM, Baratta JL, Thordarson K, Braslow J, Haynes SM, et al. Development, differentiation, and vascular components of subcutaneous and intrahepatic Hepa129 tumors in a mouse model of hepatocellular carcinoma. Histol Histopathol. 2016;31(4):403-13.
41. Xu ZT, Ding H, Fu TT, Zhu YL, Wang WP. A Nude Mouse Model of Orthotopic Liver Transplantation of Human Hepatocellular Carcinoma HCCLM3 Cell Xenografts and the Use of Imaging to Evaluate Tumor Progression. Med Sci Monit. 2019;25:8694-703.
42. Zhang Y, Lee SH, Wang C, Gao Y, Li J, Xu W. Establishing metastatic patient-derived xenograft model for colorectal cancer. Jpn J Clin Oncol. 2020.
43. Uloza V, Kuzminiene A, Palubinskiene J, Balnyte I, Uloziene I, Valanciute A. Model of human recurrent respiratory papilloma on chicken embryo chorioallantoic membrane for tumor angiogenesis research. Histol Histopathol. 2017;32(7):699-710.

44. Sommers SC, Sullivan BA, Warren S. Heterotransplantation of human cancer. III. Chorioallantoic membranes of embryonated eggs. Cancer Res. 1952;12(12):915-7.
45. Liu M, Scanlon CS, Banerjee R, Russo N, Inglehart RC, Willis AL, et al. The Histone Methyltransferase EZH2 Mediates Tumor Progression on the Chick Chorioallantoic Membrane Assay, a Novel Model of Head and Neck Squamous Cell Carcinoma. Transl Oncol. 2013;6(3):273-81.
46. Vu BT, Shahin SA, Croissant J, Fatieiev Y, Matsumoto K, Le-Hoang Doan T, et al. Chick chorioallantoic membrane assay as an in vivo model to study the effect of nanoparticle-based anticancer drugs in ovarian cancer. Sci Rep. 2018;8(1):8524.
47. Kim JS, Min J, Recknagel AK, Riccio M, Butcher JT. Quantitative three-dimensional analysis of embryonic chick morphogenesis via microcomputed tomography. Anat Rec (Hoboken). 2011;294(1):1-10.
48. Huang C, Lowerison MR, Lucien F, Gong P, Wang D, Song P, et al. Noninvasive Contrast-Free 3D Evaluation of Tumor Angiogenesis with Ultrasensitive Ultrasound Microvessel Imaging. Sci Rep. 2019;9(1):4907.
49. Siemann DW, Warrington KH, Horsman MR. Targeting tumor blood vessels: an adjuvant strategy for radiation therapy. Radiother Oncol. 2000;57(1):5-12.
50. Ribatti D, Nico B, Pezzolo A, Vacca A, Meazza R, Cinti R, et al. Angiogenesis in a human neuroblastoma xenograft model: mechanisms and inhibition by tumour-derived interferon-gamma. Br J Cancer. 2006;94(12):1845-52.
51. Kraman M, Bambrough PJ, Arnold JN, Roberts EW, Magiera L, Jones JO, et al. Suppression of antitumor immunity by stromal cells expressing fibroblast activation protein-alpha. Science. 2010;330(6005):827-30.
52. Euhus DM, Hudd C, LaRegina MC, Johnson FE. Tumor measurement in the nude mouse. J Surg Oncol. 1986;31(4):229-34.
53. Jensen MM, Jorgensen JT, Binderup T, Kjaer A. Tumor volume in subcutaneous mouse xenografts measured by microCT is more accurate and reproducible than determined by 18F-FDG-microPET or external caliper. BMC Med Imaging. 2008;8:16.
54. Wu T, Heuillard E, Lindner V, Bou About G, Ignat M, Dillenseger JP, et al. Multimodal imaging of a humanized orthotopic model of hepatocellular carcinoma in immunodeficient mice. Sci Rep. 2016;6:35230.
55. Hu J, Ishihara M, Chin AI, Wu L. Establishment of xenografts of urological cancers on chicken chorioallantoic membrane (CAM) to study metastasis. Precis Clin Med. 2019;2(3):140-51.
56. Kim Y, Williams KC, Gavin CT, Jardine E, Chambers AF, Leong HS. Quantification of cancer cell extravasation in vivo. Nat Protoc. 2016;11(5):937-48.
57. Zhu W, Jarman KE, Lokman NA, Neubauer HA, Davies LT, Gliddon BL, et al. CIB2 Negatively Regulates Oncogenic Signaling in Ovarian Cancer via Sphingosine Kinase 1. Cancer Res. 2017;77(18):4823-34.

Figures

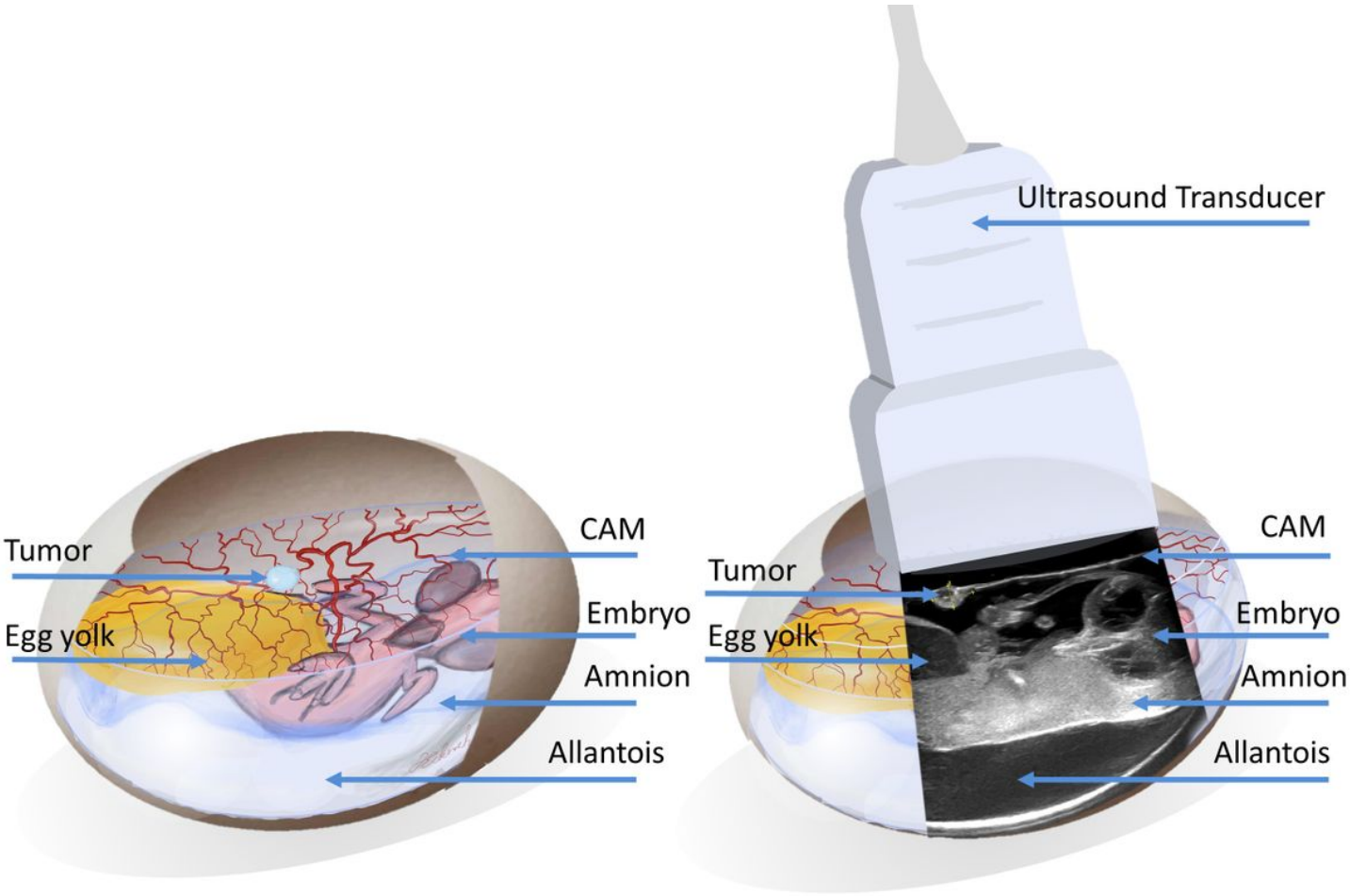

Figure 1

Visualization of the tumor and adjacent anatomical structures in ovo. Further to the ultrasonographic overview in resemblance, tumors where magnified and focused upon to allow maximum precision regarding size and vascularization measurements.

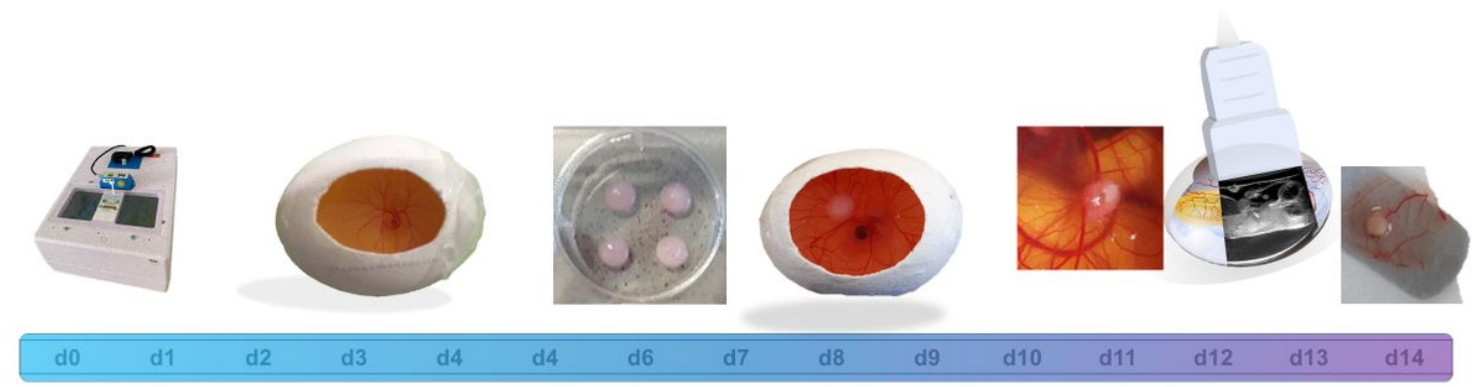

Incubation		Opening		3D Culture	Tumor Inoculation	Solid Tumor	Sonography	Fixation
Day 0		Day 3		Day 6	Day 7	Day 11	Day 12-14	Day 14
100% (n=1044)						53% n=550	54% (100/186)	

Figure 2

Timeline visualizing chronological steps of experimentation: Of the 1044 eggs evaluated, 53% (550 eggs) successfully inoculated a tumor at day 11 without any intervention. In 186 eggs with solid tumors evaluated for ultrasonographic imaging, in 100 eggs (54%) sufficient visualization was possible.

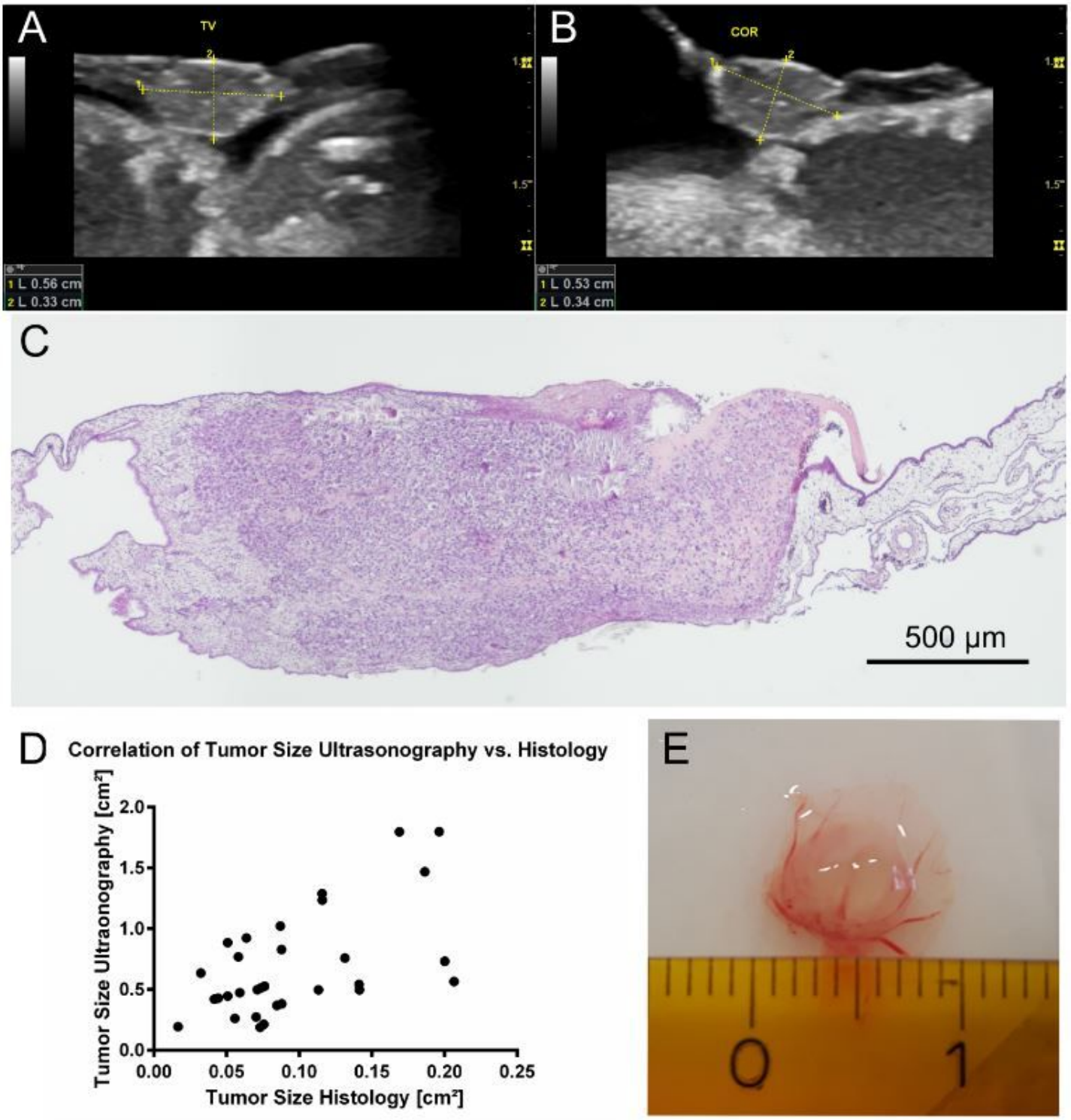

Figure 3

Ultrasonographic image of the inoculated tumor in ovo in longitudinal (A) coronar (B) plain. Image of tumor in HE staining in light microscopy (C). Correlation of tumor size determined in ultrasonography and histology (r=0.49) (D). Photographic evaluation of tumor size after excision on day 14 (E).

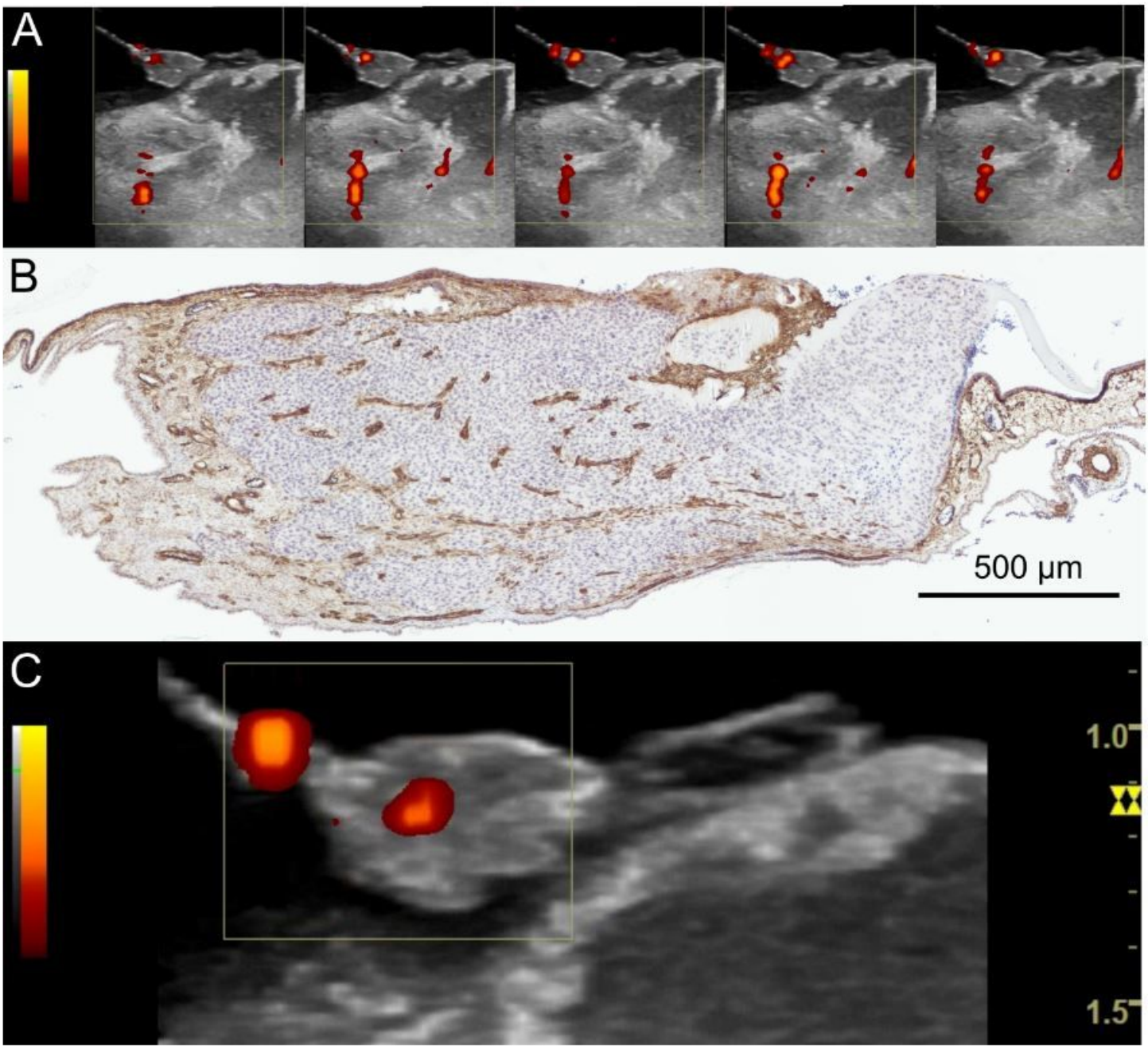

Figure 4

Image sequence of the color-duplex- ultrasonography visualizing the intratumoral blood flow as well as the blood flow in adjacent anatomical structures in ovo. (corresponding video sequence attached. See Supplementary Information S1) (A). Histological section in ASMA staining with evidence of intratumoral vessel distribution (B). Intratumoral blood flow in color-duplex-ultrasonography. (Corresponding video sequence attached. See Supplementary Information S2) (C).

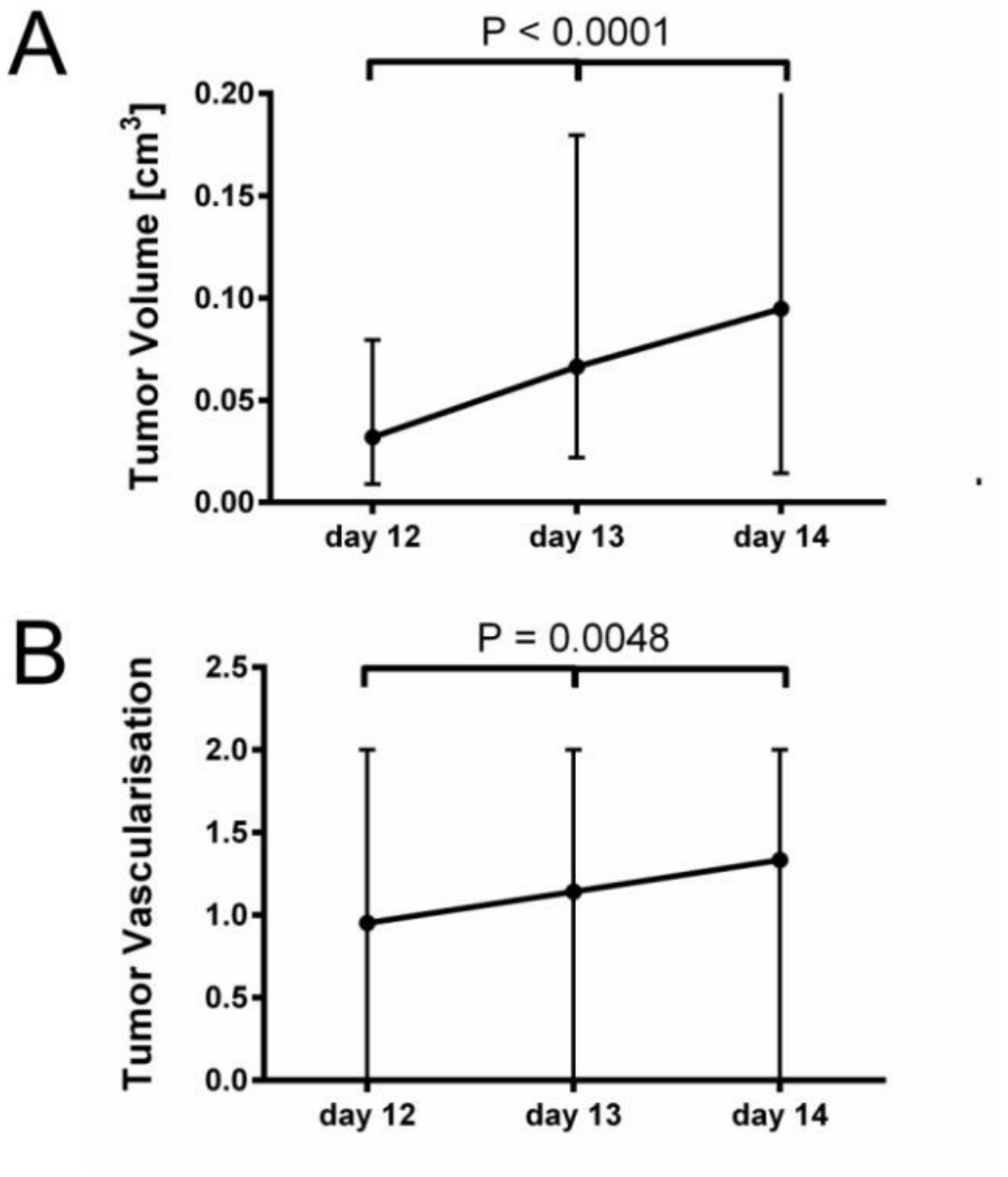

Figure 5

Average tumor growth in repetitive measurements (shown as median + range). Differences between groups were calculated using the Friedman test (A) (n= 36). Repetitive evaluation of tumor vascularization in ultrasonography (shown as median + range). Differences between groups were calculated using the Friedman test (B) (n= 36).

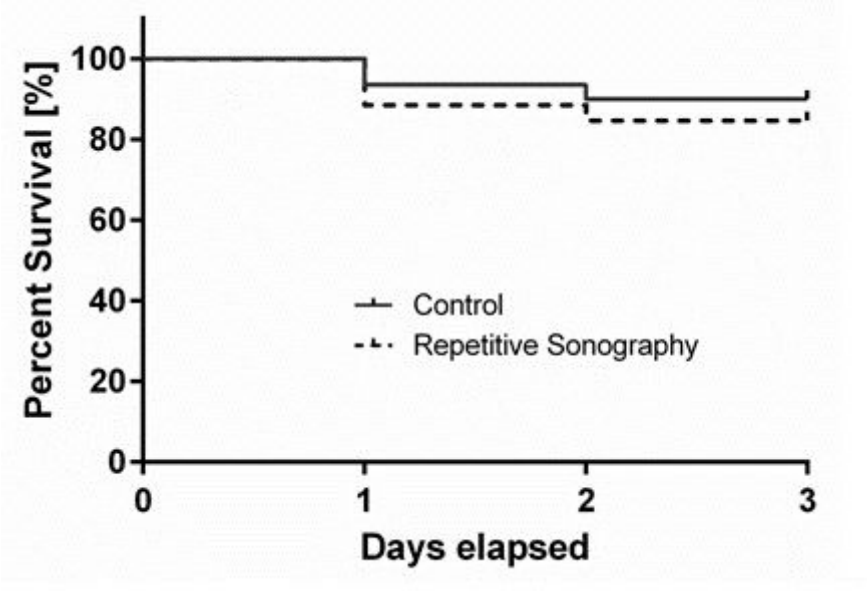

Figure 6

Kaplan Meier curve of dropout rates during the time period (day 12, 13, 14) of repetitive ultrasonography. The log-rank test as well as the Gehan-Breslow-Wilcoxon test were used to determine differences in dropout rates.

Supplementary Files

This is a list of supplementary files associated with this preprint. Click to download.

- FigureS4.tif
- FigureS4.tif
- FgS3.tif
- FgS3.tif
- SupplementaryfileS2.wmv
- SupplementaryfileS2.wmv
- SupplementaryfileS1.wmv
- SupplementaryfileS1.wmv
- SupplementaryMaterial.docx
- SupplementaryMaterial.docx